

---

# Graph Reinforcement Learning for Network Control via Bi-Level Optimization

---

Anonymous Author(s)

Anonymous Affiliation

Anonymous Email

## Abstract

Dynamic network flow models have been extensively studied and widely used in the past decades to formulate many problems with great real-world impact, such as transportation, supply chain management, power grid control, and more. Within this context, time-expansion techniques currently represent a generic approach for solving control problems over dynamic networks. However, the complexity of these methods does not allow traditional approaches to scale to large networks, especially when these need to be solved recursively over a receding horizon (e.g., to yield a sequence of actions in model predictive control). Moreover, tractable optimization-based approaches are limited to simple linear deterministic settings, and are not able to handle environments with stochastic, non-linear, or unknown dynamics. In this work, we present dynamic network flow problems through the lens of reinforcement learning and propose a graph network-based framework that can handle a wide variety of problems and learn efficient algorithms without significantly compromising optimality. Instead of a naive and poorly-scalable formulation, in which agent actions (and thus network outputs) consist of actions on edges, we present a two-phase decomposition. The first phase consists of an RL agent specifying *desired outcomes* to the actions. The second phase exploits the problem structure to solve a convex optimization problem and achieve (as best as possible) these desired outcomes. This formulation leads to dramatically improved scalability and performance. We further highlight a collection of features that are potentially desirable to system designers, investigate design decisions, and present experiments showing the utility, scalability, and flexibility of our framework.

## 1 Introduction

Many economically critical real-world systems are well-modelled through the lens of control on graphs. Power generation [1–3]; road, rail, and air transportation systems [4, 5]; complex manufacturing systems, supply chain, and distribution networks [6, 7]; telecommunication networks [8–10]; and many other systems are fundamentally the problem of controlling flows of products, vehicles, or other quantities on graph-structured networks. Traditionally, these problems are approached through the definition of a *dynamic network flow model* (DNF) [11, 12]. Within this class of problems, Ford and Fulkerson [13, 14] proposed a generic approach, showing how one can use time-expansion techniques to (i) convert dynamic networks with discrete time horizon into static networks, and (ii) solve the problem using algorithms developed for static networks. However, this approach leads to networks that grow exponentially in the input size of the problem, thus not allowing traditional methods to scale to large networks. Moreover, the design of good heuristics or approximation algorithms for network flow problems often requires significant specialized knowledge and trial-and-error.

In this paper, we argue that data-driven strategies have the potential to automate this challenging, tedious process, and learn efficient algorithms without compromising optimality. To do so, we propose a graph network-based reinforcement learning framework that can handle a wide variety of network control problems. Specifically, we introduce a bi-level formulation that leads to dramatically improved scalability and performance by combining the strengths of mathematical optimization and learning-based approaches.

## 2 Problem Setting: Dynamic Network Control

To outline our problem formulation, we first define the linear problem, which is a classic convex problem formulation. We will then define a nonlinear, dynamic, non-convex problem setting that better corresponds to real-world instances. Much of the classical flow control literature and practice substitute the former linear problem for the latter nonlinear problem to yield tractable optimization problems [15–17]; we leverage the linear problem as an important algorithmic primitive. We consider the control of  $N_c$  commodities on graphs, for example, vehicles in a transportation problem. A graph  $\mathcal{G} = \{\mathcal{V}, \mathcal{E}\}$  is defined as a set  $\mathcal{V}$  of  $N_v$  nodes, and a set  $\mathcal{E}$  of  $N_e$  ordered pairs of nodes  $(i, j)$  called edges, each described by a traversal time  $t_{ij}$ . We use  $\mathcal{N}^+(i), \mathcal{N}^-(i) \subseteq \mathcal{V}$  for the set of nodes having edges pointing away from or toward node  $i$ , respectively. We use  $s_i^t(k) \in \mathbb{R}$  to denote the quantity of commodity  $k$  at node  $i$  and time  $t$ <sup>1</sup>.

**The Linear Network Control Problem.** Within the linear model, our commodity quantities evolve in time as

$$s_i^{t+1} = s_i^t + f_i^t + e_i^t, \quad \forall i \in \mathcal{V} \quad (1)$$

where  $f_i^t$  denotes the change due to flow of commodities along edges and  $e_i^t$  denotes the change due to exchange between commodities at the same graph node. We refer to this expression as the *conservation of flow*. We also accrue money as

$$m^{t+1} = m^t + m_f^t + m_e^t, \quad (2)$$

where  $m_f^t, m_e^t \in \mathbb{R}$  denote the money gained due to flows and exchanges respectively. Money can also be replaced with any other form of scalar reward, although it may be subject to e.g. non-negativity constraints and thus is different from the notion of reward in the RL problem. Our overall problem formulation will typically be to control **flows** and **exchanges** so as to maximize money over one or more steps subject to additional constraints such as, e.g., flow limitations through a particular edge. Please refer to Appendix A for a formal treatment of flow and exchange quantities, together with practical constraints within network control problems.

**The Nonlinear Dynamic Network Control Problem.** The previous subsection presented a linear problem formulation that yields a convex optimization problem for the decision variables—the chosen flow and exchange values. However, the formulation is limited by the assumption of linearity, thus lacking in the characterization of a number of elements typical of real-world systems (please refer to Appendix A for a more complete treatment). Crucially, these nonlinear, time-varying, stochastic, or unknown elements lead to severe difficulties in applying the convex formulation derived in the previous subsection. A common approach is to solve a linearized version of the nonlinear problem at each timestep, which is a form of model predictive control (MPC), although this essentially discards some elements of the problem to achieve computational tractability. In this paper, we focus on solving the nonlinear problem (reflecting real, highly general problem statements) via a bilevel optimization approach, wherein the linear problem (which has been shown to be extremely useful in practice) is used as an inner control primitive.

## 3 Methodology: The Bi-Level Formulation

In this section we describe the bi-level formulation that is the primary contribution of this paper. We further introduce a more formal Markov decision process (MDP) for our problem setting, together with a discussion on practical elements for real-world problem formulations in Appendix B.

**The Bi-Level Formulation.** We consider a discounted infinite-horizon MDP  $\mathcal{M} = (\mathcal{S}, \mathcal{A}, P, R, \gamma)$ . Here,  $s^t \in \mathcal{S}$  is the state and  $a^t \in \mathcal{A}$  is the action space, both at time  $t$ . The state in this setting is commodity values at nodes, as well as other available information; actions corresponds to aforementioned decision variables. The dynamics,  $P : \mathcal{S} \times \mathcal{A} \times \mathcal{S} \rightarrow [0, 1]$  are probabilistic, with  $P(s^{t+1} | s^t, a^t)$  denoting a conditional distribution over  $s^{t+1}$ . The reward function  $R : \mathcal{S} \times \mathcal{A} \rightarrow \mathbb{R}$  is real-valued, and not limited to strictly positive or negative rewards. Finally, we write the discount factor as  $\gamma$  as is typical in the infinite-horizon RL formulation, although it is straightforward to instead consider a finite-horizon setting. Please refer to Appendix B.1 for further treatment of the MDP.

The overall goal of the reinforcement learning problem setting is to find a policy  $\tilde{\pi}^* \in \tilde{\Pi}$  (where  $\tilde{\Pi}$  is the space of realizable Markovian policies) such that  $\tilde{\pi}^* \in \arg \max_{\tilde{\pi} \in \tilde{\Pi}} \mathbb{E}_\tau [\sum_{t=0}^{\infty} \gamma^t R(s^t, a^t)]$ ,

<sup>1</sup>We consider several reduced views over these quantities, and maintain several notational rules. We write  $s_i^t \in \mathbb{R}^{N_c}$  to denote the vector of all commodities; we write  $s^t(k) \in \mathbb{R}^{N_v}$  to denote the vector of commodity  $k$  at all nodes; we write  $s_i(k) \in \mathbb{R}^T$  to denote commodity  $k$  at node  $i$  for all times  $t$ . We can also apply any combination of these notation rules, yielding for example  $s \in \mathbb{R}^{T \times N_c \times N_v}$ .

92 where  $\tau = (s^0, a^0, s^1, a^1, \dots)$  denotes the trajectory of states and actions. This policy formulation  
 93 requires specifying a distribution over all flow/exchange actions, which may be an extremely large  
 94 space. We instead consider a bi-level formulation

$$\pi^* \in \arg \max_{\pi \in \Pi} \mathbb{E}_{\tau} \left[ \sum_{t=0}^{\infty} \gamma^t R(s^t, a^t) \right] \quad \text{s.t. } a^t = \text{LCP}(\hat{s}^{t+1}, s^t) \quad (3)$$

95 where we consider a stochastic policy  $\pi(\hat{s}^{t+1} | s^t)$ , which maps from the current state to a *goal*  
 96 *next state* (or subset of the state, such as commodity values only). This goal next state is used in  
 97 the linear control problem ( $\text{LCP}(\cdot, \cdot)$ ), which leverages a (slightly modified) one-step version of the  
 98 linear problem formulation of Section 2 to map from desired next state to action. Thus, the resulting  
 99 formulation is a bi-level optimization problem, whereby the policy  $\tilde{\pi}$  is the composition of the policy  
 100  $\pi(\hat{s}^{t+1} | s^t)$  and the solution to the linear control problem. Specifically, given a sample of  $\hat{s}^{t+1}$  from  
 101 the stochastic policy, we select concrete flow and exchange actions by solving the linear control  
 102 problem, defined as

$$\arg \min_{a^t} d(\hat{s}^{t+1}, s^{t+1}) - R(s^t, a^t) \quad (4a)$$

$$\text{s.t. Conservation of flow (1); Net flow (5); Flow reward (6);} \quad (4b)$$

$$\text{Exchange conditions (7); Other constraints, e.g. (8) or (9)} \quad (4c)$$

103 where  $d(\cdot, \cdot)$  is a chosen convex metric which penalizes deviation from the desired next state. The  
 104 resultant problem—consisting of a convex objective subject to linear constraints—is convex and thus  
 105 may be easily and inexpensively solved to choose actions  $a^t$ , even for very large problems.

106 As is standard in reinforcement learning, we will aim to solve this problem via learning the policy  
 107 from data. This may be in the form of online learning [18] or via learning from offline data [19]. There  
 108 are large bodies of work on both problems, and our presentation will generally aim to be as-agnostic-  
 109 as-possible to the underlying reinforcement learning algorithm used. Of critical importance is the  
 110 fact that the majority of reinforcement learning algorithms use likelihood ratio gradient estimation  
 111 (typically referred to as the REINFORCE gradient estimator in RL [20]), which does not require  
 112 path-wise backpropagation through the inner problem.

113 We also note that our formulation assumes access to a model (the linear problem) that is a reasonable  
 114 approximation of the true dynamics over short horizons. This short-term correspondence is central to  
 115 our formulation: we exploit exact optimization when it is useful, and otherwise push the impacts of the  
 116 nonlinearity over time in the learned policy. We assume this model is known in our experiments, but  
 117 it could be identified independently. Please see Appendix C.1, C.2, and C.4 for a broader discussion.

118 **Network Architecture.** To exploit the network structure of the problem we introduce a policy  
 119 graph neural network architecture based on message passing neural networks [21] (Appendix B.2).  
 120 As introduced in this section, the goal of RL is to learn a stochastic policy  $\pi(\hat{s}^{t+1} | s^t)$  mapping to  
 121 goal next states. Concretely, to obtain a valid probability density over next states, we define the output  
 122 of our policy network to represent the concentration parameters  $\alpha \in \mathbb{R}_+^{N_v}$  of a Dirichlet distribution,  
 123 such that  $\hat{s}^{t+1} \sim \text{Dir}(\hat{s}^{t+1} | \alpha)$ , although alternate output formulations are possible.

## 124 4 Experiments

125 In this section, we compare against a number of benchmarks on an instance of network control with  
 126 great real-world impact: the *minimum cost flow problem*. Within this context, the goal is to control  
 127 commodities so to move them from one or more source nodes to one or more sink nodes, in the  
 128 minimum time possible. Appendix E provides further details on both benchmarks and environments.

129 **Minimum cost flow through message passing.** In this first experiment, we consider 3 different  
 130 environments (Fig. 1), such that different topologies enforce a different number of *required hops of*  
 131 *message passing* between source and sink nodes to select the best path. Results in Table 1 (*2-hop,*  
 132 *3-hop, 4-hop*) show how MPNN-RL is able to achieve at least 87% of oracle performance. Table  
 133 1 further shows how agents based on graph convolutions (i.e., GCN [22], GAT [23]) fail to learn  
 134 an effective flow optimization strategy. As in Xu et al. [24], we argue in favor of the *algorithmic*  
 135 *alignment* between the computational structure of MPNNs and the kind of computations needed to  
 136 solve traditional network optimization problems (see Appendix C.3 for further discussion).

137 **Dynamic traversal times.** In this experiment, we define time-dependent traversal times. In Fig. 2  
 138 and Table 1 (*Dyn tt*) we measure results on a dynamic network characterized by two *change-points*,  
 139 i.e., time steps where the optimal path changes because of a change in traversal times. Results show  
 140 how the proposed MPNN-RL is able to achieve above 99% of oracle performance.

**Table 1:** Average performance across multiple environments over 100 test episodes

		Random	MLP-RL	GCN-RL	GAT-RL	MPNN-RL (ours)	Oracle
2-hops	Avg. Reward	63	387	201	146	<b>576</b>	642
	% Oracle	9.9%	60.2%	31.3%	22.9%	<b>89.7%</b>	-
3-hops	Avg. Reward	1013	1084	1385	1257	<b>1803</b>	2014
	% Oracle	50.3%	53.8%	68.7%	62.4%	<b>89.5%</b>	-
4-hops	Avg. Reward	2033	2185	2303	2198	<b>2807</b>	3223
	% Oracle	63.1%	67.8%	71.4%	68.2%	<b>87.1%</b>	-
Dyn tt	Avg. Reward	-546	-18	437	400	<b>2306</b>	2327
	% Oracle	-23.4%	-0.7%	18.7%	17.1%	<b>99.1%</b>	-
Dyn top	Avg. Reward	810	N/A	1016	827	<b>1599</b>	1904
	% Oracle	42.5%	N/A	53.4%	43.4%	<b>83.9%</b>	-
Capacity	Avg. Reward	1495	1498	1557	1503	<b>2145</b>	2389
	% Oracle	62.6%	62.7%	65.2%	62.9%	<b>89.8%</b>	-
	Success Rate	82%	82%	87%	80%	<b>87%</b>	88%
Multi-com	Avg. Reward	2191	4045	3278	3206	<b>6986</b>	9701
	% Oracle	22.5%	41.7%	33.8%	33.0%	<b>72.0%</b>	-

141 **Dynamic topology.** In this experiment we assume a time-dependent topology, i.e., nodes and edges  
 142 can be dropped or added during an episode. This case is substantially different from what most  
 143 traditional approaches are able to handle: the locality of MPNN agents together with the one-step  
 144 implicit planning of RL, enable our framework to deal with multiple graph configurations during  
 145 the same episode. Fig. 3 and Table 1 (*Dyn top*) show how MPNN-RL achieves 83.9% of oracle  
 146 performance clearly outperforming the other benchmarks. Crucially, these results highlight how  
 147 agents based on MLPs result in highly inflexible network controllers, thus limited to a fixed topology.

148 **Capacity constraints.** In this experiment, we relax the assumption that capacities  $\bar{f}_{ij}$  are always  
 149 able to accommodate any flow on the graph. Compared to previous sections, the lower capacities  
 150 introduce the possibility of infeasible states. To measure this, the *Success Rate* computes the  
 151 percentage of episodes which have been terminated successfully. Results in Table 1 (*Capacity*)  
 152 highlight how MPNN-RL is able to achieve 89.8% of oracle performance while being able to  
 153 successfully terminate 87% of episodes. Qualitatively, Fig. 4 shows a visualization of the policy for a  
 154 specific test episode. The plots show how the MPNN-RL is able to learn the effects of capacity on the  
 155 optimal strategy by allocating flow to a different node when the corresponding edge is approaching  
 156 its capacity limit.

157 **Multi-commodity.** In this scenario, we extend the current architecture to deal with multiple  
 158 commodities and source-sink combinations. Results in Table 1 (*Multi-com*) and Fig. 5 show how  
 159 MPNN-RL is able to effectively recover distinct policies for each policy head, thus being able to  
 160 operate successfully multi-commodity flows within the same network.

161 **Computational analysis.** We study the computational cost of MPNN-RL compared to MPC-based  
 162 solutions. As shown in Fig. 6, we compare the time necessary to compute a single network flow  
 163 decision. We do so across varying dimensions of the underlying graph, ranging from 10 up to 400  
 164 nodes. As verified by this experiment, learning-based approaches exhibit computational complexity  
 165 linear in the number of nodes and graph connectivity, without significant decay in performance.

## 166 5 Outlook and Limitations

167 Research in network flow models, in both theory and practice, is largely scattered across the control,  
 168 management science, and optimization literature, potentially hindering scientific progress. In this  
 169 work, we propose a general framework that could enable learning-based approaches to help address  
 170 the open challenges in this space: handling nonlinear dynamics and scalability, among others. In  
 171 the hope of fostering a unification of tools among the reinforcement learning and network control  
 172 communities, we aimed to (i) maintain the narration as-agnostic-as-possible, and (ii) showcase the  
 173 extreme versatility of our framework through numerous controlled experiments. However, what  
 174 we present here should be considered as, in our opinion, exciting preliminary results aiming to  
 175 gather more traction among the ML community towards the solution of hugely impactful real-world  
 176 problems in the field of network control. Crucially, before being able to consider learning-based  
 177 frameworks as a concrete alternative to current standards, we believe this research opens several  
 178 promising future directions for the extension of these concepts to large-scale applications.

## References

- 179  
180 [1] Daniel Bienstock, Michael Chertkov, and Sean Harnett. Chance-constrained optimal power  
181 flow: Risk-aware network control under uncertainty. *SIAM Review*, 56(3):461–495, 2014. 1
- 182 [2] Hermann W Dommel and William F Tinney. Optimal power flow solutions. *IEEE Transactions*  
183 *on power apparatus and systems*, (10):1866–1876, 1968.
- 184 [3] M Huneault and Francisco D Galiana. A survey of the optimal power flow literature. *IEEE*  
185 *transactions on Power Systems*, 6(2):762–770, 1991. 1
- 186 [4] Y. Wang, W. Y. Szeto, K. Han, and T. Friesz. Dynamic traffic assignment: A review of  
187 the methodological advances for environmentally sustainable road transportation applications.  
188 *Transportation Research Part B: Methodological*, 111:370–394, 2018. 1
- 189 [5] D. Gammelli, K. Yang, J. Harrison, F. Rodrigues, F. C. Pereira, and M. Pavone. Graph neural  
190 network reinforcement learning for autonomous mobility-on-demand systems. In *Proc. IEEE*  
191 *Conf. on Decision and Control*, 2021. 1, 10
- 192 [6] Haralambos Sarimveis, Panagiotis Patrinos, Chris D Tarantilis, and Chris T Kiranoudis. Dy-  
193 namic modeling and control of supply chain systems: A review. *Computers & operations*  
194 *research*, 35(11):3530–3561, 2008. 1
- 195 [7] Marcus A Bellamy and Rahul C Basole. Network analysis of supply chain systems: A systematic  
196 review and future research. *Systems Engineering*, 16(2):235–249, 2013. 1
- 197 [8] Gabriel Jakobson and Mark Weissman. Real-time telecommunication network management:  
198 Extending event correlation with temporal constraints. In *International Symposium on Integrated*  
199 *Network Management*, pages 290–301, 1995. 1
- 200 [9] John Edward Flood. *Telecommunication networks*. IET, 1997.
- 201 [10] Vladimir Popovskij, Alexander Barkalov, and Larysa Titarenko. *Control and adaptation in*  
202 *telecommunication systems: Mathematical Foundations*, volume 94. Springer Science &  
203 Business Media, 2011. 1
- 204 [11] R. K. Ahuja, T. L. Magnanti, and J. B. Orlin. *Network Flows: Theory, Algorithms and*  
205 *Applications*. Prentice Hall, 1993. 1
- 206 [12] B. Kotnyek. An annotated overview of dynamic network flows. *INRIA*, 2003. 1
- 207 [13] L. R. Ford and D. R. Fulkerson. Constructing maximal dynamic flows from static flows.  
208 *Operations Research*, 6(3):419–433, 1958. 1
- 209 [14] L. R. Ford and D. R. Fulkerson. *Flows in Networks*. Princeton Univ. Press, 1962. 1
- 210 [15] Fangxing Li and Rui Bo. Dcopf-based lmp simulation: algorithm, comparison with acopf, and  
211 sensitivity. *IEEE Transactions on Power Systems*, 22(4):1475–1485, 2007. 2
- 212 [16] Rick Zhang, Federico Rossi, and Marco Pavone. Model predictive control of autonomous  
213 mobility-on-demand systems. In *2016 IEEE International Conference on Robotics and Automa-*  
214 *tion (ICRA)*, pages 1382–1389, 2016.
- 215 [17] Peter B Key and Graham A Cope. Distributed dynamic routing schemes. *IEEE Communications*  
216 *Magazine*, 28(10):54–58, 1990. 2
- 217 [18] R. S. Sutton and A. G. Barto. *Reinforcement Learning: An Introduction*. MIT Press, 2 edition,  
218 2018. 3, 11
- 219 [19] S. Levine, A. Kumar, G. Tucker, and J. Fu. Offline reinforcement learning: Tutorial, review,  
220 and perspectives on open problems. *arXiv:2005.01643*, 2020. 3
- 221 [20] R.-J. Williams. Simple statistical gradient-following algorithms for connectionist reinforcement  
222 learning. *Machine Learning*, 1992. 3
- 223 [21] Gilmer J., Schoenholz S., Riley P., Vinyals O., and Dahl G. Neural message passing for quantum  
224 chemistry. In *Int. Conf. on Machine Learning*, 2017. 3
- 225 [22] T.-N. Kipf and M. Welling. Semi-supervised classification with graph convolutional networks.  
226 In *Int. Conf. on Learning Representations*, 2017. 3
- 227 [23] P. Veličković, G. Cucurull, A. Casanova, A. Romero, O. Liò, and Y. Bengio. Graph attention  
228 networks. In *Int. Conf. on Learning Representations*, 2018. 3
- 229 [24] K. Xu, J. Li, M. Zhang, S. Du, K. Kawarabayashi, and S. Jegelka. What can neural networks  
230 reason about? In *Int. Conf. on Learning Representations*, 2020. 3
- 231 [25] H. Markowitz. Portfolio selection. *Journal of Finance*, 7(1):77–91, 1952. 10

- 232 [26] H. U. Gerber and G. Pafum. Utility functions: From risk theory to finance. *North American*  
233 *Actuarial Journal*, 2(3):74–91, 1998. 10
- 234 [27] V. Konda and J. Tsitsiklis. Actor-critic algorithms. In *Conf. on Neural Information Processing*  
235 *Systems*, 1999. 10
- 236 [28] V. Mnih, K. Kavukcuoglu, D. Silver, A. Rusu, et al. Human-level control through deep  
237 reinforcement learning. *Nature*, 518(7540):529–533, 2015. 10
- 238 [29] V. Mnih, A. Puigdomenech, M. Mirza, A. Graves, T.-P. Lillicrap, T. Harley, D. Silver, and  
239 K. Kavukcuoglu. Asynchronous methods for deep reinforcement learning. In *Int. Conf. on*  
240 *Learning Representations*, 2016. 10
- 241 [30] D. Gammelli, K. Yang, J. Harrison, F. Rodrigues, F. C. Pereira, and M. Pavone. Graph meta-  
242 reinforcement learning for transferable autonomous mobility-on-demand. In *ACM Int. Conf. on*  
243 *Knowledge Discovery and Data Mining*, 2022. 10
- 244 [31] K. Murota. *Matrices and Matroids for Systems Analysis*. Springer Science & Business Media, 1  
245 edition, 2009. 10
- 246 [32] Mario VF Pereira and Leontina MVG Pinto. Multi-stage stochastic optimization applied to  
247 energy planning. *Mathematical Programming*, 52(1):359–375, 1991. 11
- 248 [33] Justin Dumouchelle, Rahul Patel, Elias B Khalil, and Merve Bodur. Neur2sp: Neural two-stage  
249 stochastic programming. *arXiv:2205.12006*, 2022. 11
- 250 [34] Scott Fujimoto, David Meger, Doina Precup, Ofir Nachum, and Shixiang Shane Gu. Why should  
251 i trust you, bellman? the bellman error is a poor replacement for value error. *arXiv:2201.12417*,  
252 2022. 11
- 253 [35] A. Shapiro, D. Dentcheva, and A. Ruszczyński. *Lectures on stochastic programming: Modeling*  
254 *and theory*. SIAM, second edition, 2014. 11, 12
- 255 [36] J. Rawlings and D. Mayne. *Model predictive control: Theory and design*. Nob Hill Publishing,  
256 2013. 12
- 257 [37] Tom Van de Wiele, David Warde-Farley, Andriy Mnih, and Volodymyr Mnih. Q-learning in  
258 enormous action spaces via amortized approximate maximization. *arXiv:2001.08116*, 2020. 12
- 259 [38] C. Finn, P. Abbeel, and S. Levine. Model-agnostic meta-learning for fast adaptation of deep  
260 networks. In *Int. Conf. on Machine Learning*, 2017. 12
- 261 [39] James Harrison, Apoorva Sharma, and Marco Pavone. Meta-learning priors for efficient online  
262 bayesian regression. In *Workshop on Algorithmic Foundations of Robotics*, pages 318–337,  
263 2018.
- 264 [40] A. Agrawal, S. Barratt, S. Boyd, E. Busseti, and W. M. Moursi. Differentiating through a conic  
265 program. Online, 2019.
- 266 [41] A. Agrawal, S. Barratt, S. Boyd, and B. Stellato. Learning convex optimization control policies.  
267 In *Learning for Dynamics & Control*, 2019. 12, 13
- 268 [42] B. Amos and J. Z. Kolter. Optnet: Differentiable optimization as a layer in neural networks. In  
269 *Int. Conf. on Machine Learning*, 2017.
- 270 [43] Benoit Landry, Joseph Lorenzetti, Zachary Manchester, and Marco Pavone. Bilevel optimization  
271 for planning through contact: A semidirect method. In *The International Symposium of Robotics*  
272 *Research*, pages 789–804, 2019.
- 273 [44] Luke Metz, Niru Maheswaranathan, Jeremy Nixon, Daniel Freeman, and Jascha Sohl-Dickstein.  
274 Understanding and correcting pathologies in the training of learned optimizers. In *Int. Conf. on*  
275 *Machine Learning*, pages 4556–4565, 2019. 12
- 276 [45] Aviv Tamar, Garrett Thomas, Tianhao Zhang, Sergey Levine, and Pieter Abbeel. Learning  
277 from the hindsight plan—episodic mpc improvement. In *Proc. IEEE Conf. on Robotics and*  
278 *Automation*, pages 336–343, 2017. 12
- 279 [46] Brandon Amos, Ivan Jimenez, Jacob Sacks, Byron Boots, and J Zico Kolter. Differentiable  
280 mpc for end-to-end planning and control. *Conf. on Neural Information Processing Systems*, 31,  
281 2018. 12, 13
- 282 [47] Brian Ichter, James Harrison, and Marco Pavone. Learning sampling distributions for robot  
283 motion planning. In *Proc. IEEE Conf. on Robotics and Automation*, pages 7087–7094, 2018. 12
- 284 [48] Thomas Power and Dmitry Berenson. Variational inference mpc using normalizing flows and  
285 out-of-distribution projection. *arXiv:2205.04667*, 2022.

- 286 [49] Brandon Amos and Denis Yarats. The differentiable cross-entropy method. In *Int. Conf. on*  
287 *Machine Learning*, pages 291–302, 2020. [12](#)
- 288 [50] Jacob Sacks and Byron Boots. Learning to optimize in model predictive control. In *Proc. IEEE*  
289 *Conf. on Robotics and Automation*, pages 10549–10556, 2022. [12](#)
- 290 [51] Xuesu Xiao, Tingnan Zhang, Krzysztof Marcin Choromanski, Tsang-Wei Edward Lee, Anthony  
291 Francis, Jake Varley, Stephen Tu, Sumeet Singh, Peng Xu, Fei Xia, Leila Takayama, Roy  
292 Frostig, Jie Tan, Carolina Parada, and Vikas Sindhwani. Learning model predictive controllers  
293 with real-time attention for real-world navigation. In *Conf. on Robot Learning*, 2022. [12](#)
- 294 [52] Priya Donti, Brandon Amos, and J Zico Kolter. Task-based end-to-end model learning in  
295 stochastic optimization. *Conf. on Neural Information Processing Systems*, 30, 2017. [13](#)
- 296 [53] Peter W Glynn. Likelihood ratio gradient estimation for stochastic systems. *Communications*  
297 *of the ACM*, 33(10):75–84, 1990. [13](#)
- 298 [54] A. Paszke, S. Gross, F. Massa, A. Lerer, et al. Pytorch: An imperative style, high-performance  
299 deep learning library. *arXiv preprint arXiv:1912.01703*, 2019. [13](#)
- 300 [55] IBM. *ILOG CPLEX User's guide*. IBM ILOG, 1987. [13](#)
- 301 [56] R. Zhang, F. Rossi, and M. Pavone. Model predictive control of Autonomous Mobility-on-  
302 Demand systems. In *Proc. IEEE Conf. on Robotics and Automation*, 2016. [13](#)

## 303 A Dynamic Network Control

304 In this section we make concrete both our linear and nonlinear problem formulation.

305 **Flows.** We will denote flows along edge  $(i, j)$  with  $f_{ij}^t(k)$ . From these flows, we have

$$f_i^t = \sum_{j \in \mathcal{N}^-(i)} f_{ji}^t - \sum_{j \in \mathcal{N}^+(i)} f_{ij}^t, \quad \forall i \in \mathcal{V} \quad (5)$$

306 which is the net flow (inflows minus outflows). As discussed, associated with each flow is a cost  
 307  $m_{ij}^t(k)$ . Note that given this formulation, the total cost for all commodities can be written as  
 308  $m_{ij}^t \cdot f_{ij}^t = (m_{ij}^t)^\top f_{ij}^t$ . Thus, we can write the total flow cost at time  $t$  as

$$m_f^t = \sum_{i \in \mathcal{V}} \left( \sum_{j \in \mathcal{N}^-(i)} m_{ji}^t \cdot f_{ji}^t - \sum_{j \in \mathcal{N}^+(i)} m_{ij}^t \cdot f_{ij}^t \right). \quad (6)$$

309 **Exchanges.** To define our exchange relations and their effect on commodity quantities and costs,  
 310 we will write the effect which exchanges have on money for each node; we write this as  $m_i^t$ . Thus,  
 311 we have  $m_e^t = \sum_{i \in \mathcal{V}} m_i^t$ . The exchange relation takes the form

$$\begin{bmatrix} e_i^t \\ m_i^t \end{bmatrix} = E_i^t w_i^t \quad (7)$$

312 where  $E_i^t \in \mathbb{R}^{N_c+1 \times N_e(i)}$  is an exchange matrix and  $w \in \mathbb{R}^{N_e(i)}$  are the weights for each exchange.  
 313 Each column in this exchange matrix denotes an (exogenous) exchange rate between commodities;  
 314 for example, for  $i$ 'th column  $[-1, 1, 0.1]^\top$ , one unit of commodity one is exchanged for one unit of  
 315 commodity two plus 0.1 units of money. Thus, choice of exchange weights  $w_i^t$  uniquely determines  
 316 exchanges  $e_i^t$  and money change due to exchanges,  $m_e^t$ .

317 **Linear Constraints.** We may impose additional (linear) constraints on the problem beyond the  
 318 conservation of flow we have discussed so far. There are a few common examples that we may use in  
 319 several applications. A common constraint is non-negativity of commodity values, which we may  
 320 express as

$$s_i^t \geq 0, \quad \forall i, t. \quad (8)$$

321 Note that this inequality is defined element-wise. A similar constraint can be defined for money. We  
 322 may also impose constraints on flows and exchanges; thus, we may for example limit the flow of all  
 323 commodities through a particular edge via

$$\sum_{k=1}^{N_c} f_{ij}^t(k) \leq \bar{f}_{ij}^t \quad (9)$$

324 where this sum could also be weighted per-commodity. These linear constraints are only a limited  
 325 selection of some common examples; the space of possible constraints is extremely general and the  
 326 particular choice of constraints is problem-specific.

327 **Elements breaking the linearity assumptions.** Real-world systems are characterized by many  
 328 factors that cannot be reliably modelled through the linear problem described in Section 2. In what  
 329 follows, we discuss a (non-exhaustive) list of factors potentially breaking such linearity assumptions:

- 330 • **Stochasticity.** Various stochastic elements can impact the problem. Commodity transitions in  
 331 the previous section were defined as being deterministic; in practice in many problems, there are  
 332 elements of stochasticity to these transitions. For example, random demand may reduce supply  
 333 by an unpredictable amount; vehicles may be randomly added in a transportation problem; and  
 334 packages may be lost in a supply chain setting. In addition to these state transitions, constraints  
 335 may be stochastic as well: flow times or edge capacities may be stochastic, as when a road is  
 336 shared with other users, or costs for flows and exchange may be stochastic.
- 337 • **Nonlinearity.** Various elements of the state evolution, constraints, or cost function may be  
 338 nonlinear. The objective may be chosen to be a risk-sensitive or robust metric applied to the  
 339 distribution of outcomes, as is common in financial problems. The state evolution may have  
 340 natural saturating behavior (e.g. automatic load shedding). Indeed, many real constraints will  
 341 have natural nonlinear behavior.



- 342 • **Time-varying costs and constraints.** Similar to the stochastic case, various quantities may  
343 be time-varying. However, it is possible that they are time-varying in a structured way, as  
344 opposed to randomly. For example, demand for transportation may vary over the time of day, or  
345 purchasing costs may vary over the year.
- 346 • **Unknown dynamics elements.** While not a major focus of discussion in the paper up to  
347 this point, elements of the underlying dynamics may be partially or wholly unknown. Our  
348 reinforcement learning formulation is capable of addressing this by learning policies directly  
349 from data, in contrast to standard control techniques.

## 350 B Methodology

351 In this section we discuss the full MDP formulation (including defining state and action spaces) and  
352 discuss algorithmic details.

### 353 B.1 The Dynamic Network MDP

354 The problem setting for the full, dynamic network problem is best formulated, in the general case,  
355 as a partially-observed MDP. We will present it as a Markovian decision process (fully-observed),  
356 where the choice of input features beyond commodity values are chosen by the user; discussion on  
357 strategies for better handling partial-observability are presented later in this section.

358 We consider a discounted infinite-horizon MDP  $\mathcal{M} = (\mathcal{S}, \mathcal{A}, P, R, \gamma)$ . Here,  $s^t \in \mathcal{S}$  is the state  
359 and  $a^t \in \mathcal{A}$  is the action space, both at time  $t$ . The dynamics,  $P : \mathcal{S} \times \mathcal{S} \times \mathcal{A} \rightarrow [0, 1]$  are  
360 probabilistic, with  $P(s^{t+1} | s^t, a^t)$  denoting a conditional distribution over  $s^{t+1}$ . The reward  
361 function  $R : \mathcal{S} \times \mathcal{A} \rightarrow \mathbb{R}$  is real-valued, and not limited to strictly positive or negative rewards.  
362 Finally, we write the discount factor as  $\gamma$  as is typical in the infinite-horizon RL formulation, although  
363 it is straightforward to instead consider a finite-horizon setting.

364 **State and state space.** We will, generally, define the state to contain enough information to yield  
365 “good” Markovian policies. More formally, real-world network control problems are typically highly  
366 partially-observed; many features of the world impact the state evolution. However, a small number of  
367 features are typically of primary importance, and the impact of the other partially-observed elements  
368 can be modeled as stochastic disturbances.

369 For our bi-level formulation, there are some state elements that are required. Our formulation requires,  
370 at each timestep, the commodity values  $s^t$ . Furthermore, the constraint values are required, such as  
371 costs, exchange rates, flow capacities, etc. If the graph topology is time-varying, the connectivity  
372 at time  $t$  is also critical. The state values to fully define the one-step linear control problem are the  
373 only state elements which are required. We refer to these constraint values as edge state elements.  
374 More precisely, the state elements we have discussed so far are either properties of the graph nodes  
375 (commodity values) or of the edges (such as flow constraints). This difference is of critical importance  
376 in our graph neural network architecture.

377 In addition to these state elements, additional information may be incorporated. Generally, the  
378 choice of state elements will depend on the information available to a system designer (what can  
379 be measured) and will depend on the particular problem setting. Possible examples of further state  
380 elements include forecasts of prices, exchange rates, or flow constraints at future times; exchanges  
381 rates, for example, include notions of demand or supply. We note that such forecasts are almost  
382 always available, as they are necessary for solving the multi-step planning problem.

383 **Action and action space.** As discussed in Section 2, the action is defined as all flows and exchange  
384 weights at all nodes/edges,  $a^t = (f^t, w^t)$ . In our bi-level formulation, we compute  $a^t$  by replacing a  
385 single policy mapping from states to actions with two nested policies, whereby the goal next state  
386  $s^{t+1}$  acts as an intermediate variable, thus avoiding the parametrization of an extremely large action  
387 space, e.g., flows over edges in a graph. Specifically, the goal next state is fed into a linear control  
388 problem (LCP) to obtain the edge-wise flows that would best match the desired next state. Thus, the  
389 policy for the original problem is defined as a composition of policies.

390 **Dynamics.** The dynamics of the MDP,  $P$ , describe the evolution of state elements. We split our  
391 discussion in to two parts: the dynamics associated with the commodity time evolution and the  
392 dynamics of the non-commodity elements.

393 The commodity dynamics are assumed to be reasonably well-modeled by the conservation of flow,  
394 (1), subject to the constraints; this forms the basis of the bi-level approach we describe in the next  
395 subsection. The primary element not included in the conservation of flow expression is possible  
396 stochasticity. For example, in transportation problems, vehicles may randomly drop out of service.

397 The non-commodity dynamics are assumed to be substantially more complex. For example, prices  
 398 to buy or sell (reflected in exchange rates) may have a complex dependency on past sales, current  
 399 demand, and current supply (commodity values), as well as random exogenous factors. Thus, we  
 400 place few assumptions on the evolution of non-commodity dynamics, and assume that current values  
 401 are measurable.

402 **Reward.** Throughout the paper, we will assume our full reward is the total discounted money earned  
 403 over the (infinite) problem duration. This results in a stage-wise reward function that corresponds  
 404 simply to the money earned in that time period, or

$$R(s^t, a^t) = m_e^t + m_f^t. \quad (10)$$

405 Note that the sum of rewards to time  $t$  is exactly  $m^t - m^0$ , which corresponds to the money earned.  
 406 It is typical in economics and finance to consider concave utility functions or risk metrics as opposed  
 407 to the exact return [25, 26]. However, this reward structure does not result in a simple stage-wise  
 408 reward decomposition as in the linear case. Thus, while addressing this concavity is important, we do  
 409 not address it in this work.

## 410 B.2 Network Architecture and RL Details

411 In this section we introduce the basic building blocks of our graph neural network architecture. Let  
 412 us define with  $\mathbf{x}_i \in \mathbb{R}^{D_x}$  and  $\mathbf{e}_{ji} \in \mathbb{R}^{D_e}$  the  $D_x$ -dimensional vector of node features of node  $i$  and  
 413 the  $D_e$ -dimensional vector of edge features from node  $j$  to node  $i$ , respectively.

414 We define the update function of node features through the following message passing neural network  
 415 (MPNN):

$$\mathbf{x}_i^{(k)} = \max_{j \in \mathcal{N}^-(i)} f_\theta \left( \mathbf{x}_i^{(k-1)}, \mathbf{x}_j^{(k-1)}, \mathbf{e}_{ji} \right), \quad (11)$$

416 where  $k$  indicates the  $k$ -th layer of message passing in the GNN with  $k = 0$  indicating raw envi-  
 417 ronment features, i.e.,  $\mathbf{x}_i^{(0)} = \mathbf{x}_i$ , and where we use the element-wise max operator as aggregation  
 418 function in our proposed graph-network.

419 We note that this network architecture can be used to define both policy and value function estimator,  
 420 depending on the reinforcement learning algorithm of interest (e.g., actor-critic [27], value-based  
 421 [28], etc.). As an example, in our implementation, we define two separate decoder architectures  
 422 for the actor and critic networks of an Advantage Actor Critic (A2C) [29] algorithm. For the actor,  
 423 we define the output of our policy network to represent the concentration parameters  $\alpha \in \mathbb{R}_+^{N_v}$  of a  
 424 Dirichlet distribution, such that  $\mathbf{a}_t \sim \text{Dir}(\mathbf{a}_t | \alpha)$ , and where the positivity of  $\alpha$  is ensured by a Softplus  
 425 nonlinearity. On the other hand, the critic is characterized by a *global* sum-pooling performed after  
 426  $K$  layers of MPNN. In this way, the critic computes a single value function estimate for the entire  
 427 network by aggregating information across all nodes in the graph.

428 **Handling dynamic topologies.** A defining property of our framework is its ability to deal with  
 429 time-dependent graph connectivity (e.g., edges or nodes are added/dropped during the course of an  
 430 episode). Specifically, our framework achieves this by (i) considering the problem as a one-step  
 431 decision-making problem, i.e., avoiding the dependency on potentially unknown future topologies,  
 432 and (ii) exploiting the capacity of GNNs to handle diverse graph topologies. Crucially, no matter  
 433 the current state of the graph, GNN-based agents are capable of computing a goal next state for the  
 434 network, which will then be converted into actionable flow decisions by the LCP.

435 **Exploration.** In practice, we choose large penalty terms  $d(\cdot, \cdot)$  to minimize greediness. However  
 436 early in training, randomly initialized penalty terms can harm exploration. In practice, we found it  
 437 was sufficient to down-weight the penalty term early in training. As such, the inner action selection  
 438 is biased toward short-term rewards, resulting in greedy action selection. However, there are many  
 439 further possibilities for exploiting random penalty functions to induce exploration, which we discuss  
 440 in the next section.

441 **Integer-valued flows.** For several problem settings, it is desirable that the chosen flows be *integer-*  
 442 *valued*. For example, in a transportation problem, we may wish to allocate some number of vehicles,  
 443 which can not be infinitely sub-divided [5, 30]. There are several ways to introduce integer-valued  
 444 constraints to our framework. First, we note that because the RL agent is trained through policy  
 445 gradient—and thus we do not require a differentiable inner problem—we can simply introduce integer  
 446 constraints into the lower-level problem<sup>2</sup>. However, solving integer-constrained problems is typically

<sup>2</sup>Note that several problems exhibit a *total unimodularity* property [31], for which the relaxed integer-valued problem is tight.

447 expensive in practice. An alternate solution is to simply use a heuristic rounding operation on the  
 448 output of the inner problem. Again, because of the choice of gradient estimator, this does not need  
 449 to be differentiable. Moreover, the RL policy learns to adapt to this heuristic clipping. Thus, we in  
 450 general recommend this strategy as opposed to directly imposing constraints in the inner problem.

## 451 C Discussion and Algorithmic Components

452 In this section we discuss various elements of the proposed framework, highlight correspondences  
 453 and design decisions, and discuss component-level extensions.

### 454 C.1 Distance metric as value function

455 The role of the distance metric (and the generated goal next state) is to capture the value of future  
 456 reward in the greedy one-step inner optimization problem. This is closely related to the value function  
 457 in dynamic programming and reinforcement learning, which in expectation captures the sum of future  
 458 rewards for a particular policy. Indeed, under moderate technical assumptions, our linear problem  
 459 formulation with stochasticity yields convex expected cost-to-go (the negative of the value) [32, 33].

460 There are several critical differences between our penalty term and a learned value function. First, a  
 461 value function in a Markovian setting for a given policy is a function solely of state. For example, in  
 462 the LCP, a value function would depend only on  $s^{t+1}$ . In contrast, our value function depends on  
 463  $\hat{s}^{t+1}$ , which is the output of a policy which takes  $s^t$  as an input. Thus, the penalty term is a function  
 464 of both the current and predicted next state. Given this, the penalty term is better understood as a  
 465 local approximation of the value function, for which convex optimization is tractable, or as a form of  
 466 state-action value function with a reduced action space (also referred to as a Q function).

467 The second major distinction between the penalty term and a value function is particular to rein-  
 468 forcement learning. Value functions in modern RL are typically learned via minimizing the Bellman  
 469 residual [18], although there is disagreement on whether this is a desirable objective [34]. In contrast,  
 470 our policy is trained directly via gradient descent on the total reward (potentially incorporating  
 471 value function control variates). Thus, the objective for this penalty method is better aligned with  
 472 maximizing total reward.

### 473 C.2 Beyond a single-step inner problem

474 Our formulation so far has considered a bi-level formulation in which the RL policy outputs a desired  
 475 state at the *next* timestep,  $\hat{s}^{t+1}$ ; this is then used in the lower-level problem to select actions. There  
 476 are two relaxations to this procedure that can be incorporated here.

477 First, the RL policy can output any future state, and direct optimization can happen for any horizon.  
 478 We may parameterize the RL policy to return  $\hat{s}^{t+k}$  for  $k \geq 1$ . Given this, a multi-step optimization  
 479 problem may be solved using the linear model. The potential risk to this approach is the linear (in  
 480 horizon) growth in variables for the inner problem, and poor agreement between the linear model  
 481 and the nonlinear model. This presents a strict generalization of our proposed method. The primary  
 482 reason we have not considered the multi-step formulation as the primary algorithm of this paper is  
 483 that it requires modeling the dynamics of the non-commodity state variables. For example, this model  
 484 requires forecasting all constraint values, whereas our one-step formulation requires only knowledge  
 485 at the current timestep. Forecasting of constraint values is closely linked to questions of (persistent)  
 486 feasibility, which we do not consider in detail in this paper.

487 Second, stochasticity may be directly integrated into the lower-level problem. The standard formula-  
 488 tion for stochastic model predictive control (or stochastic multi-stage optimization) is the scenario  
 489 formulation [35], in which a tree of outcomes is constructed via sampling noise realizations<sup>3</sup>. Within  
 490 the one-step bi-level formulation, sampling  $N_n$  noise realizations results in  $N_n$  values of the next  
 491 state,  $s_i^{t+1}$ ,  $i = 1, \dots, N_n$  within the inner problem. The empirical mean loss

$$\mathbb{E}_{s^{t+1}}[d(\hat{s}^{t+1}, s^{t+1})] - R(s^t, a^t) \approx \frac{1}{N_n} \sum_{i=1}^{N_n} d(\hat{s}^{t+1}, s_i^{t+1}) - R(s^t, a^t) \quad (12)$$

492 can then be minimized. We emphasize that the actions are the same for each noise realization—this  
 493 is the so-called *non-anticipativity* constraint. This formulation, for one step, does not meaningfully  
 494 increase the number of decision variables, although will result in increased computational complexity.

<sup>3</sup>We note that non-sampling strategies such as moment-matching formulations are also possible, although we will not discuss these methods herein.

495 More importantly, multi-step optimization within the scenario tree approach yields exponential  
 496 growth in the number of decision variables, which will rapid result in intractability. We refer the  
 497 reader to [35] for more details on scenario-based stochastic optimization.

### 498 C.3 Graph neural networks for network optimization

499 In this work, we argue that GNNs represent a natural choice for graph optimization problems because  
 500 of three main properties:

501 First, permutation invariance, or, more specifically, GNNs represent a class of functions for which  
 502 the output is independent of the node ordering. Crucially, non-permutation invariant computations  
 503 would consider each ordering as fundamentally different and thus require an exponential number of  
 504 input/output training examples before being able to generalize.

505 Second, locality of the operator. GNNs typically express a local parametric filter (e.g., convolution  
 506 operator) which enables the same neural network to be applied to graphs of varying size and connec-  
 507 tivity: a property of fundamental importance for network flow optimization problems specifically, and  
 508 real-world problems of economic importance more generally, which will be dynamic or frequently  
 509 re-configured, and it is desirable to be able to use the same policy without re-training.

510 Lastly, alignment with the computations used for network optimization problems. The concept of  
 511 algorithmic alignment refers to the fact that despite many neural network architectures have the  
 512 *capacity* to represent a wide range of algorithms, not all networks are able to actually *learn* these  
 513 algorithms. Intuitively, a network may learn and generalize better if it is able to represent a function  
 514 (algorithm) “more easily.” A notable example of this in the context of supervised learning is the  
 515 relation between MLPs and CNNs in computer vision—where MLPs are theoretically universal  
 516 approximators yet struggle to achieve satisfying performance on most vision tasks. The difference in  
 517 results of MLP-RL in Table 1 (2-hops) compared to Table 1 (3-hops, 4-hops) further confirms these  
 518 concepts, whereby the smaller dimensionality of the 2-hops environment leads to a smaller solution  
 519 space for the MLPs, which are able to converge to relatively good policies. On the other hand, the  
 520 3-hops and 4-hops environments are characterized by a significant increase in the number of edges  
 521 and nodes, leading to a more challenging search for solutions in policy-space.

### 522 C.4 Computational efficiency

523 Consider solving the full nonlinear control problem via direct optimization over a finite horizon ( $T$   
 524 timesteps), which corresponds to a model predictive control [36] formulation. How many total actions  
 525 must be selected? The number of possible flows for a fully dense graph (worst case) is  $N_v(N_v - 1)$ .  
 526 In addition to this, there are  $\sum_{i \in \mathcal{V}} N_e(i)$  possible exchange actions; if we assume  $N_e$  is the same for  
 527 all nodes, this yields  $N_v N_e$  possible actions. Finally, we have  $N_c$  commodities. Thus, the worst-case  
 528 number of actions to select is  $T N_c N_v (N_v + N_e - 1)$ ; it is evident that for even moderate choices of  
 529 each variable, the complexity of action selection in our problem formulation quickly grows beyond  
 530 tractability.

531 While moderately-sized problems may be tractable within the direct optimization setting, we aim  
 532 to incorporate the impacts of stochasticity, nonlinearity, and uncertainty, which typically results in  
 533 non-convexity. The reinforcement learning approach, in addition to being able to improve directly  
 534 from data, reduces the number of actions required to those for a single step. If we were to directly  
 535 parameterize the naive policy that outputs flows and exchanges, this would correspond to  $N_c N_v (N_v +$   
 536  $N_e - 1)$  actions. For even moderate values of  $N_c, N_v, N_e$ , this can result in millions of actions. It  
 537 is well-known that reinforcement learning algorithms struggle with high dimensional action spaces  
 538 [37], and thus this approach is unlikely to be successful. In contrast, our bi-level formulation requires  
 539 only  $N_c$  actions for the learned policy, while additionally leveraging the beneficial inductive biases  
 540 over short time horizons.

## 541 D Related Work

542 Bi-level optimization—in which one optimization problem depends on the solution to another  
 543 optimization problem, and are thus nested—has recently become an important topic in machine  
 544 learning, reinforcement learning, and control [38–44]. Of particular relevance to our framework  
 545 are methods that combine principled control strategies with learned components in a hierarchical  
 546 way. Examples include using LQR control in the inner problem with learnable cost and dynamics  
 547 [41, 45, 46]; learning sampling distributions in planning and control [47–49]; or learning optimization  
 548 strategies or goals for optimization-based control [50, 51].

549 Numerous strategies for learning control with bi-level formulations have been proposed. A simple  
 550 approach is to insert intermediate goals to train lower-level components, such as imitation [47]. This

551 approach is inherently limited by the choice of the intermediate objective; if this objective does  
 552 not strongly correlate with the downstream task, learning could emphasize unnecessary elements  
 553 or miss critical ones. An alternate strategy, which we take in this work, is directly optimizing  
 554 through an inner controller. A large body of work has focused on exploiting exact solutions to  
 555 the gradient of (convex) optimization problems at fixed points [41, 46, 52]. This allows direct  
 556 backpropagation through optimization problems, allowing them to be used as a generic component  
 557 in a differentiable computation graph (or neural network). Our approach leverages likelihood ratio  
 558 gradients (equivalently, policy gradient), an alternate zeroth-order gradient estimator [53]. This  
 559 enables easy differentiation through lower-level optimization problems without the technical details  
 560 necessitated with fixed-point differentiation.

## 561 E Experiments

### 562 E.1 Benchmarks

563 All RL modules were implemented using PyTorch [54] and the IBM CPLEX solver [55] for the  
 564 optimization problem. In our experiments, we compare the proposed framework with the following  
 565 methods:

566 **Heuristics.** In this class of methods, we focus on measuring performance of simple, domain-  
 567 knowledge-driven rebalancing heuristics.

- 568 1. *Random policy*: at each timestep, we sample the desired distribution from a Dirichlet prior  
 569 with concentration parameter  $\alpha = [1, 1, \dots, 1]$ . This benchmark provides a lower bound of  
 570 performance by choosing desired goal states randomly.

571 **Learning-based.** Within this class of methods, we focus on measuring how different architectures  
 572 affect the quality of the solutions for the dynamic network control problem. For all methods, the A2C  
 573 algorithm is kept fixed, thus the difference solely lies in the neural network architecture.

- 574 3. *MLP-RL*: both policy and value function estimator are parametrized by feed-forward neural  
 575 networks. In all our experiments, we use two layers of 32 hidden units and an output layer  
 576 mapping to the output's support (e.g., a scalar value for the critic network). Through this  
 577 comparison, we highlight the performance and flexibility of graph representations for network-  
 578 structured data.
- 579 4. *GCN-RL*: In all our experiments, we use  $K$  layers of graph convolution with 32 hidden units,  
 580 with  $K$  equal to the number of sink-to-source hops in the graph, and a linear output layer  
 581 mapping to the output's support. See below for a broader discussion of graph convolution  
 582 operators.
- 583 5. *GAT-RL*: In all our experiments, we use  $K$  layers of graph attention with 32 hidden units, with  
 584  $K$  equal to the number of sink-to-source hops in the graph, and single attention head. The output  
 585 is further computed by a linear output layer mapping to the output's support. Together with  
 586 GCN-RL, this model represents an approach based on graph convolutions rather than explicit  
 587 message passing along the edges (as in MPNNs). Through this comparison, we argue in favor  
 588 of explicit, pair-wise messages along the edges, opposed to sole aggregation of node features  
 589 among a neighborhood. Specifically, we argue in favor of the alignment between MPNN and  
 590 the kind of computations required to solve flow optimization tasks, e.g., propagation of travel  
 591 times and selection of best path among a set of candidates (max aggregation).
- 592 6. *MPNN-RL*: ours. We use  $K$  layers of MPNN of 32 hidden units as defined in Section B.2, with  
 593  $K$  equal to the number of sink-to-source hops in the graph, and a linear output layer mapping to  
 594 the output's support.

595 **MPC-based.** Within this class of methods, we focus on measuring performance of MPC approaches  
 596 that serve as state-of-art benchmarks for the dynamic network flow problem.

- 597 5. *MPC-Oracle*: we directly optimize the flow using a standard formulation of MPC [56]. Notice  
 598 that although the embedded optimization is a linear programming model, it may not meet the  
 599 computation requirement of real-time applications (e.g., obtaining a solution within several  
 600 seconds) for large scale networks. In this work, MPC is assumed to have access to future  
 601 state elements (e.g., future traversal times, connectivity, etc.). Crucially, assuming knowledge  
 602 of future state elements is equivalent to assuming oracle knowledge of the realization of all  
 603 stochastic elements in the system. In other words, there is no uncertainty for the MPC (this  
 604 is in contrast with RL-based benchmarks, that assume access only to *current* state elements).  
 605 In our experiments, the benchmark with the "Oracle" MPC enables us to quantify the optimal

606 solution for all environments, thus giving a sense of the optimality gap between the ground truth  
 607 optimum and the solution achieved via RL.

## 608 E.2 Environments

609 In what follows, we describe the properties of the environments used to train and evaluate our  
 610 framework in order to make them reproducible and understandable. We select environment variables  
 611 in a way to cover a wide enough range of possible scenarios, e.g., different traversal times and thus,  
 612 different optimal actions.

- **Generalities.** As discussed in Section 4, the environments describe a dynamic minimum cost flow problem, whereby the goal is to let commodities flow from source to sink nodes in the minimum time possible (i.e., cost is equal to time). Formally, given a graph  $\mathcal{G} = \{\mathcal{V}, \mathcal{E}\}$ , the reward function across all environments is defined as:

$$R(s^t, a^t) = - \sum_{ij \in \mathcal{E}} f_{ij}^t t_{ij} + \lambda f_{\text{sink}}^t,$$

613 where  $f_{ij}^t$  and  $t_{ij}$  represent flow and traversal time along edge  $(i, j)$  at time  $t$ , respectively,  $f_{\text{sink}}^t$   
 614 is the flow arriving at all sink nodes at time  $t$ , and  $\lambda$  is a weighting factor between the two reward  
 615 terms. In our experiments, the resulting policy proved to be broadly insensitive to values of  $\lambda$ ,  
 616 with  $\lambda \in [15, 30]$  typically being an effective range.

- **Minimum cost flow through message passing.** Given a single-source, single-sink network, we assume travel times to be constant over the episode and requirements (i.e., demand) to be sampled at each time step as  $\rho = 10 + \psi_i, \psi_i \sim \text{Uniform}[-2, 2]$ . Capacities  $u_{ij}$  are fixed to a very high positive number, thus not representing a constraint in practice. Cost  $m_{ij}$  is considered equal to the traversal time  $t_{ij}$ . An episode is assumed to have a duration of 30 time steps and terminates when there is no more flow traversing the network. To present a variety of scenarios to the agent at training time, we sample random travel times for each new episode as  $t_{ij} \sim \text{Uniform}[0, 10]$  and use the topologies shown in Fig. 1. In our experiments, we apply as many layers of message passing as hops from source to sink node in the graph, e.g.,  $K = 2$  and  $K = 3$  in the 2-hops and 3-hops environment, respectively.
- **Dynamic traversal times.** To train our MPNN-RL, we select the 3-hops environment and generate travel times as follows for every episode: (i) sample random traversal times as  $t_{ij} \sim \text{Uniform}[0, 10]$ , (ii) for every time step, gradually change the traversal time as  $t_{ij} = t_{ij} + \psi, \psi \sim \text{Uniform}[-1, 1]$ .
- **Capacity constraints.** In this experiment, we focus on the 3-hops environment and assume a constant value  $\bar{f}_{ij} = 20, \forall i, j \in \mathcal{V} : j \neq 7$  while we keep a high value for all the edges going into node 7 (i.e., the sink node) which would more easily generate infeasible scenarios. From an RL perspective, we add the following edge-level features:
  - Edge-capacity  $\{\bar{f}_{ij}^t\}_{i,j \in \mathcal{V}}$  at the current time step  $t$ .
  - Accumulated flow  $\{f_{ij}^t\}_{i,j \in \mathcal{V}}$  on edge  $ij$
- **Multi-commodity.** Let  $N_c$  define the number of commodities to consider, indexed by  $k$ . From an RL perspective, we extend our proposed policy graph neural network to represent a  $N_c$ -dimensional Dirichlet distribution. Concretely, we define the output of the policy network to represent the  $N_c \times N_v$  concentration parameters  $\alpha \in \mathbb{R}_+^{N_c \times N_v}$  of a Dirichlet distribution over nodes for each commodity, such that  $\mathbf{a}_t \sim \text{Dir}\{\mathbf{a}_t | \alpha\}$ . In other words, to extend our approach to the multi-commodity setting, we define a multi-head policy network characterized by one head per commodity. In our experiments, we train our multi-head agent on the topology shown in Fig. 5 whereby we assume two parallel commodities: commodity A going from node 0 to node 10, and commodity B going from node 0 to node 11. We choose this topology so that the only way to solve the scenario is to discover distinct behaviours between the two network heads (i.e., the policy head controlling flow for commodity A needs to go up or it won't get any reward, and vice-versa for commodity B).
- **Computational analysis.** In this experiment, we generate different versions of the 3-hops environment, whereby different environments are characterized by intermediate layers with increasing number of nodes and edges. The results are computed by applying the pre-trained MPNN-RL agent on the original 3-hops environment (i.e., characterized by 8 nodes in the graph). In light of this, Figure 6 showcases a promising degree of transfer and generalization among graphs of different dimensions.

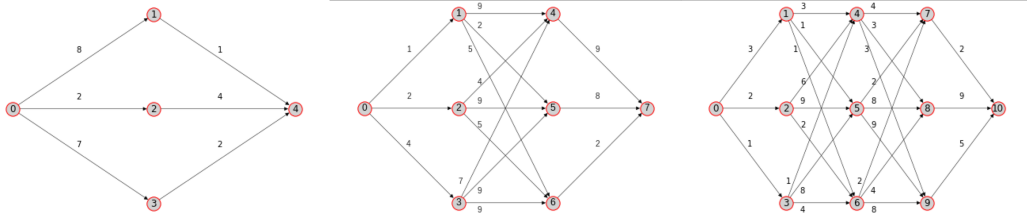


**Figure 1:** Graph topologies used for the message passing experiments: 2-hops (left), 3-hops (center), 4-hops (right). The source and sink nodes are represented by the left-most and right-most nodes, respectively. Values in proximity of the edges represent traversal times.

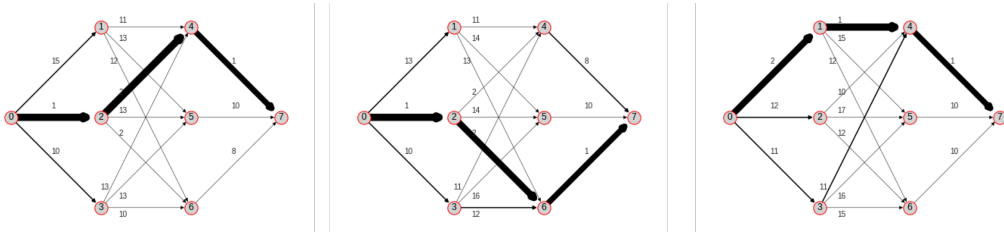


**Figure 2:** Visualization of a trained instance of MPNN-RL on an environment with dynamic traversal times. We simulate a scenario where the optimal path changes three times (left, middle, and right) over the course of an episode. Shaded edges represent actions induced by the MPNN-RL.

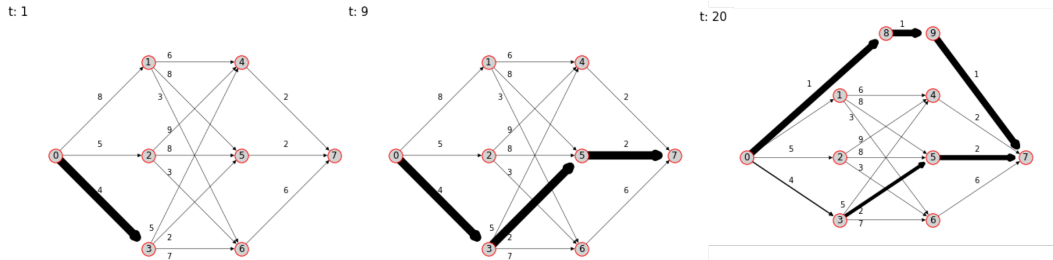


**Figure 3:** Visualization of a trained instance of MPNN-RL on an environment with dynamic topology. We simulate a scenario where the optimal path changes over the course of an episode because of the addition of a new path. Shaded edges represent actions induced by the MPNN-RL.

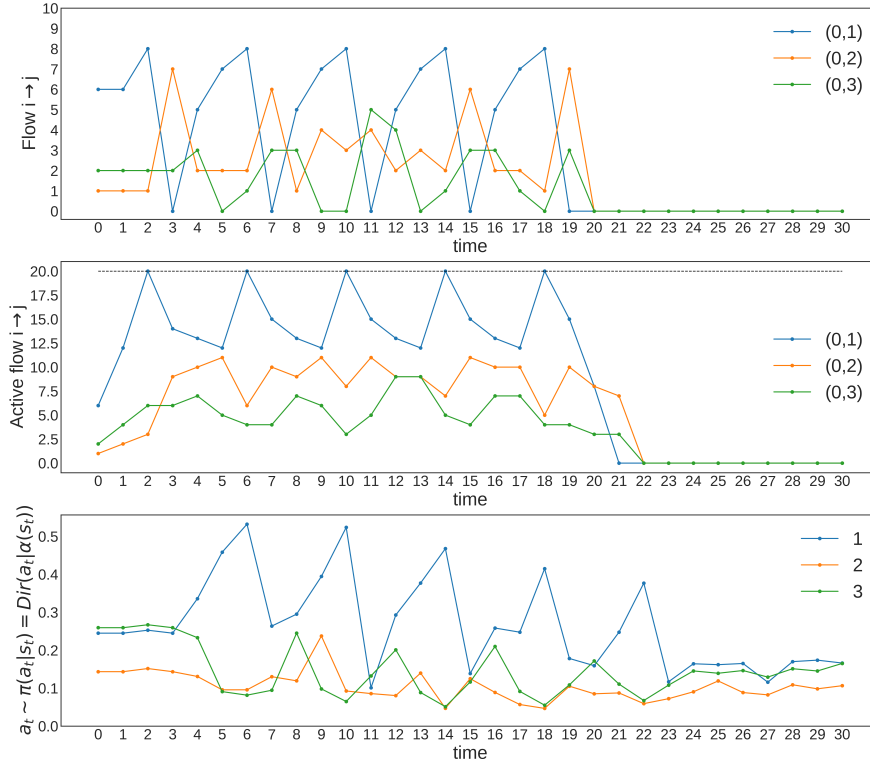


**Figure 4:** Visualization of the MPNN-RL policy on the capacity constrained environment. (Top) The resulting flow  $f_{ij}$  on the edges  $0 \rightarrow 1, 0 \rightarrow 2, 0 \rightarrow 3$ . (Center) The accumulated flow on the same edges compared to the fixed capacity  $\bar{f}_{ij} = 20$ , represented as a dashed horizontal line. (Bottom) The desired distribution described by the MPNN-RL policy.

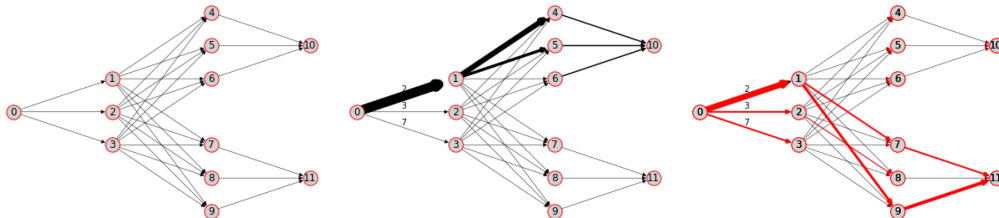


**Figure 5:** Visualization of the multi-commodity environment. (Left) The topology considered during our experiments. (Center) A visualization of the policy for the first commodity A. (Right) A visualization of the policy for the second commodity B.



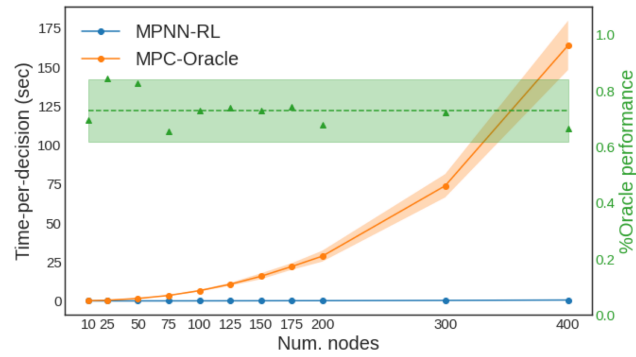


**Figure 6:** Comparison of computation times between learning-based (blue) and control-based (orange) approaches. Green triangles represent the percentage performance of our RL framework compared to the oracle model.